

# Muon $g - 2$ , Dark Matter Detection and Accelerator Physics

R. Arnowitt, B. Dutta, B. Hu and Y. Santoso

*Center For Theoretical Physics, Department of Physics, Texas A&M University, College Station  
TX 77843-4242  
(February, 2001)*

## Abstract

We examine the recently observed deviation of the muon  $g - 2$  from the Standard Model prediction within the framework of gravity mediated SUGRA models with R parity invariance. Universal soft breaking (mSUGRA) models, and models with non-universal Higgs and third generation squark/slepton masses at  $M_G$  are considered. All relic density constraints from stau-neutralino co-annihilation and large  $\tan\beta$  NLO corrections for  $b \rightarrow s\gamma$  decay are included, and we consider two possibilities for the light Higgs:  $m_h > 114$  GeV and  $m_h > 120$  GeV. The combined  $m_h$ ,  $b \rightarrow s\gamma$  and  $a_\mu$  bounds give rise to lower bounds on  $\tan\beta$  and  $m_{1/2}$ , while the lower bound on  $a_\mu$  gives rise to an upper bounds on  $m_{1/2}$ . These bounds are sensitive to  $A_0$ , e.g. for  $m_h > 114$  GeV, the 95% C.L. is  $\tan\beta > 7(5)$  for  $A_0 = 0(-4m_{1/2})$ , and for  $m_h > 120$  GeV,  $\tan\beta > 15(10)$ . The positive sign of the  $a_\mu$  deviation implies  $\mu > 0$ , eliminating the extreme cancellations in the dark matter neutralino-proton detection cross section so that almost all the SUSY parameter space should be accessible to future planned detectors. Most of the allowed parts of parameter space occur in the co-annihilation region where  $m_0$  is strongly correlated with  $m_{1/2}$ . The lower bound on  $a_\mu$  then greatly reduces the allowed parameter space. Thus using 90% C. L. bounds on  $a_\mu$  we find for  $A_0 = 0$  that  $\tan\beta \geq 10$  and for  $\tan\beta \leq 40$  that  $m_{1/2} = (290 - 550)$  GeV and  $m_0 = (70 - 300)$  GeV. Then the tri-lepton signal and other SUSY signals would be beyond the Tevatron Run II (except for the light Higgs), only the  $\tilde{\tau}_1$  and  $h$  and (and for part of the parameter space) the  $\tilde{e}_1$  will be accessible to a 500 GeV NLC, while the LHC would be able to see the full SUSY mass spectrum.

The remarkable accuracy with which the muon gyromagnetic ratio can be measured makes it an excellent probe for new physics beyond the Standard Model. The recently reported result of the Brookhaven E821 experiment now gives a  $2.6\sigma$  deviation from the predicted value of the Standard Model [1]:

$$a_\mu^{\text{exp}} - a_\mu^{\text{SM}} = 43(16) \times 10^{-10} \quad (1)$$

where  $a_\mu = (g_\mu - 2)/2$ . Efforts were made initially to calculate a possible deviation from the Standard Model within the framework of global supersymmetry (SUSY) [2]. However, one may show that in the limit of exact global supersymmetry,  $a_\mu^{\text{SUSY}}$  will vanish [3], and thus one needs broken supersymmetry to obtain a non-zero result. The absence of a phenomenologically viable way of spontaneously breaking global supersymmetry made realistic predictions for these models difficult. In contrast, spontaneous breaking of supersymmetry in supergravity (SUGRA) is easy to achieve, and the advent of supergravity grand unified models [4] led to the first calculations of  $a_\mu^{\text{SUGRA}}$  [5,6], of which [6] was the first complete analysis. Since that time there have been a number of papers updating that result. (See e.g. [7].)

In SUGRA models, the spontaneous breaking of supersymmetry triggers the Higgs VEV and hence the breaking of  $SU(2) \times U(1)$ , relating then these two mass scales. Thus the scale of the new SUSY masses is predicted to be  $\sim 100$  GeV - 1 TeV. It was then possible to predict in [6] that the SUGRA contributions would be comparable or larger than the electroweak contribution,  $15.2(4) \times 10^{-10}$  [8], in accord with the now observed deviation of Eq. (1). This scale for the SUSY masses was further confirmed by the LEP data showing that consistency with grand unification could be obtained if the SUSY masses also lie in the above range [9]. Finally, we note that SUGRA models with R-parity invariance predict a dark matter candidate (the lightest neutralino) with the astronomically observed amount of relic density if the SUSY masses again lie in this range.

It is thus reasonable to investigate whether the observed deviation from  $a_\mu^{\text{exp}}$  can be understood within the framework of SUGRA models, and in this paper we consider gravity mediated SUSY breaking with R-parity invariance for models with universal soft breaking masses (mSUGRA) and also models with non-universal masses in the Higgs and third generation sector. SUGRA models have a wide range of applicability including cosmological phenomena and accelerator physics, and constraints in one area affect predictions in other areas. In particular, as first observed in [5] and emphasized in [10], that  $a_\mu$  increases with  $\tan\beta$ , as do dark matter detection rates. Thus as we will see, the deviation of Eq. (1) will significantly effect the minimum neutralino -proton cross section,  $\sigma_{\tilde{\chi}_1^0-p}$ , for terrestrial detectors. Even more significant is the fact that the astronomical bounds on the  $\tilde{\chi}_1^0$  relic density restrict the SUSY parameter space and hence the SUGRA predictions for  $a_\mu$  as well as what may be expected to be seen at the Tevatron RUN II and the LHC. In order to carry out this analysis, however, it is necessary to include all the co-annihilation effects for large  $\tan\beta$ , as well as the large  $\tan\beta$  corrections to  $m_b$  and  $m_\tau$  (which are needed to correctly determine the corresponding Yukawa coupling constants) and the large  $\tan\beta$  NLO corrections to the  $b \rightarrow s\gamma$  decay [11]. In addition, the light Higgs ( $h$ ) mass bounds play an important role in limiting the SUSY parameter space and it is necessary to include the one and two loop corrections, and the pole mass corrections. The above corrections for dark matter (DM) calculations were carried out in [12], and we will use the same corrections here.

Recently several papers have appeared analysing the SUGRA contribution to  $a_\mu$  in light of the final LEP bounds on  $m_h$  and the deviation of Eq.(1) [13–16]. Relic density constraints were not considered in Refs. [15,16] and coannihilation effects apparently not included in Refs. [13,14]. Also Refs. [13,15,16] do not seem to have included the constraints from the  $b \rightarrow s\gamma$  decay. As will be seen below, these effects are of major importance in determining the SUGRA predictions.

Before proceeding on, we state the range of parameters we assume. We take a  $2\sigma$  bound of Eq. (1),

$$11 \times 10^{-10} < a_\mu^{\text{SUGRA}} < 75 \times 10^{-10}, \quad (2)$$

a  $2\sigma$  bound on the  $b \rightarrow s\gamma$  branching ratio,  $1.8 \times 10^{-4} < BR(b \rightarrow s\gamma) < 4.5 \times 10^{-4}$ , and a neutralino relic density range of  $0.02 < \Omega_{\tilde{\chi}_1^0} h^2 < 0.25$ . (Assuming a lower bound of 0.1 does not affect results significantly.) The  $b$ -quark mass is assumed to have the range  $4.0 \text{ GeV} < m_b(m_b) < 4.4 \text{ GeV}$ . We consider two bounds on the Higgs mass:  $m_h > 114 \text{ GeV}$  and  $m_h > 120 \text{ GeV}$ . The first is the current LEP bound and the second is likely within reach of the Tevatron Run II. However, the theoretical calculations of  $m_h$  have still some uncertainty as well as uncertainty in the  $t$ -quark mass, and so we will conservatively interpret these bounds to mean that our theoretical values obey  $m_h > 111 \text{ GeV}$  and  $117 \text{ GeV}$  respectively. (Our calculations of  $m_h$  are consistent with [17].) The scalar and gaugino masses at the GUT scale obey  $(m_0, m_{1/2}) < 1 \text{ TeV}$ . We examine the range  $2 < \tan \beta < 40$ , and the cubic soft breaking mass is parameterized at the GUT scale by  $|A_0| < 4m_{1/2}$ . Non-universal masses deviate from universality according to  $m_0^2(1 + \delta)$  where  $-1 < \delta < +1$ . Other parameters are as in [12].

We consider first the mSUGRA model, which depends on the four parameters  $m_0, m_{1/2}, A_0, \tan \beta = \langle H_2 \rangle / \langle H_1 \rangle$  (where  $\langle H_{(1,2)} \rangle$  give rise to  $(d, u)$  quark masses) and the sign of the  $\mu$  parameter of the Higgs mixing part of the superpotential ( $W = \mu H_1 H_2$ ). The SUSY contribution to  $a_\mu$  arises from two types of loop diagrams, i. e. those with chargino-sneutrino intermediate states, and those with neutralino-smuon intermediate states. The dominant contribution arises from the former term with the light chargino ( $\tilde{\chi}_1^\pm$ ). For moderate or large  $\tan \beta$ , and when  $(\mu \pm \tilde{m}_2)^2 \ll M_W^2$ , one finds

$$a_\mu^{\text{SUGRA}} \cong \frac{\alpha}{4\pi} \frac{1}{\sin^2 \theta_W} \left( \frac{m_\mu^2}{m_{\tilde{\chi}_1^\pm \mu}} \right) \frac{\tan \beta}{1 - \frac{\tilde{m}_2^2}{\mu^2}} \left[ 1 - \frac{M_W^2}{\mu^2} \frac{1 + 3\frac{\tilde{m}_2^2}{\mu^2}}{\left(1 - \frac{\tilde{m}_2^2}{\mu^2}\right)^2} \right] F(x) \quad (3)$$

where  $\tilde{m}_i = (\alpha_i/\alpha_G)m_{1/2}$ ,  $i = 1, 2, 3$  are the gaugino masses at the electroweak scale and  $\alpha_G \cong 1/24$  is the GUT scale gauge coupling constant. (One has  $m_{\tilde{\chi}_1^\pm} \cong \tilde{m}_2 \cong 0.8m_{1/2}$ , and the gluino ( $\tilde{g}$ ) mass is  $m_{\tilde{g}} \cong \tilde{m}_3$ .) In Eq. (3), the form factor is  $F(x) = (1 - 3x)(1 - x)^{-2} - 2x^2(1 - x)^{-3} \ln x$ , where  $x = (m_{\tilde{\nu}}/m_{\tilde{\chi}_1^\pm})^2$ . The sneutrino and chargino masses being related to  $m_0$  and  $m_{1/2}$  by the renormalization group equations (RGE) [18]. (The contribution from the heavy chargino,  $\tilde{\chi}_2^\pm$  reduces this result by about a third.) One finds for large  $m_{1/2}$  that  $F(x) \cong 0.6$  so that  $a_\mu$  decreases as  $1/m_{1/2}$ , while for large  $m_0$ ,  $F$  decreases as  $\ln(m_0^2)/m_0^2$  (exhibiting the SUSY decoupling phenomena).

Eq. (3) exhibits also the fact discussed in [10,19] that the sign of  $a_\mu^{\text{SUGRA}}$  is given by the sign of  $\mu$ . Eq. (1) thus implies that  $\mu$  is positive (as pointed out in [14–16]). This then

has immediate consequences for dark matter detection. Thus as discussed in [20,21,12], for  $\mu < 0$ , accidental cancellations can occur reducing the neutralino-proton cross section to below  $10^{-10}$  pb over a wide range of SUSY parameters, and making halo neutralino dark matter unobservable for present or future planned terrestrial detectors. Thus this possibility has now been eliminated, and future detectors (e.g. GENIUS) should be able to scan almost the full SUSY parameter space for  $m_{1/2} < 1$  TeV.

The lower bound of Eq. (1) plays a central role in limiting the  $\mu > 0$  SUSY parameter space, particularly when combined with the bounds on the Higgs mass and the  $b \rightarrow s\gamma$  constraints. As seen above, lowering  $\tan\beta$  can be compensated in  $a_\mu$  by also lowering  $m_{1/2}$ . However,  $m_h$  decreases with both decreasing  $\tan\beta$  and decreasing  $m_{1/2}$ . Thus the combined Higgs and  $a_\mu$  bounds put a lower bound on  $\tan\beta$ . This bound is sensitive to  $A_0$  since  $A_0$  enters in the L-R mixing in the stop (mass)<sup>2</sup> matrix and affects the values of the stop masses. We find for  $m_h > 111$  GeV (i.e. the 114 GeV experimental bound), that  $\tan\beta > 7$  for  $A_0 = 0$ , and  $\tan\beta > 5$  for  $A_0 = -4m_{1/2}$ . At higher  $m_h$  the bound on  $\tan\beta$  is more restrictive. Thus for  $m_h > 117$  GeV (corresponding to an experimental 120 GeV bound), one has  $\tan\beta > 15$  for  $A_0 = 0$ , and  $\tan\beta > 10$  for  $A_0 = -4m_{1/2}$ . As the Higgs mass increases, the bound on  $\tan\beta$  increases. As discussed in [22,12,23,21], for large  $\tan\beta$ , the relic density constraints leave only co-annihilation regions possible, and these are very sensitive to the value of  $A_0$ . Fig. 1 exhibits the allowed regions in the  $m_0 - m_{1/2}$  plane for  $\tan\beta = 40$ ,  $m_h > 111$  GeV for  $A_0 = 0, -2m_{1/2}$ , and  $4m_{1/2}$  (from bottom to top). The corridors terminate at low  $m_{1/2}$  due to the  $b \rightarrow s\gamma$  and  $m_h$  constraints. Without the  $a_\mu$  constraint, the corridors would extend up to the end of the parameter space ( $m_{1/2} = 1$  TeV). We see also that the relic density constraint effectively determines  $m_0$  in terms of  $m_{1/2}$  in this region. The lower bound of Eq. (1), however, cuts off these curves (at the verticle lines) preventing  $m_0$  and  $m_{1/2}$  from getting too large. Thus for large  $\tan\beta$ , the  $g_\mu - 2$  experiment puts a strong constraint on the SUSY parameter space.

The restriction of the SUSY parameter space by the  $a_\mu$  constraint affects the predicted dark matter detection rates. Thus the exclusion of the large  $m_0$  and large  $m_{1/2}$  domain of Fig. 1 generally raises the lower bounds on the neutralino-proton cross section. In Fig. 2 we have plotted  $\sigma_{\tilde{\chi}_1^0-p}$  as a function of  $m_{\tilde{\chi}_1^0}$  for  $\tan\beta = 40$  for the allowed corridors for  $A_0 = -2m_{1/2}, 4m_{1/2}$  and 0 (bottom to top). The curves terminate at high  $m_{\tilde{\chi}_1^0}$  due to the lower bound on  $a_\mu$  of Eq. (1). (Note that  $m_{\tilde{\chi}_1^0} \cong 0.4m_{1/2}$ .) Again one sees the sensitivity of results to the value of  $A_0$ , both for the high  $m_{\tilde{\chi}_1^0}$  termination point and for the magnitude of the cross section. Over the full range one has that  $\sigma_{\tilde{\chi}_1^0-p} > 6 \times 10^{-10}$  pb, and hence should generally be accessible to future planned detectors.

## FIGURES

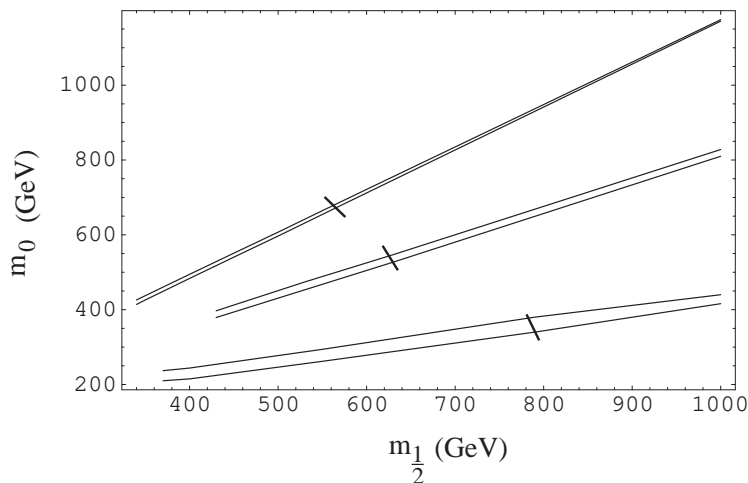


FIG. 1. Corridors in the  $m_0 - m_{1/2}$  plane allowed by the relic density constraint for  $\tan\beta = 40$ ,  $m_h > 111$  GeV,  $\mu > 0$  for  $A_0 = 0, -2m_{1/2}, 4m_{1/2}$  from bottom to top. The curves terminate at low  $m_{1/2}$  due to the  $b \rightarrow s\gamma$  constraint except for the  $A_0 = 4m_{1/2}$  which terminates due to the  $m_h$  constraint. The short lines through the allowed corridors represent the high  $m_{1/2}$  termination due to the lower bound on  $a_\mu$  of Eq. (1).

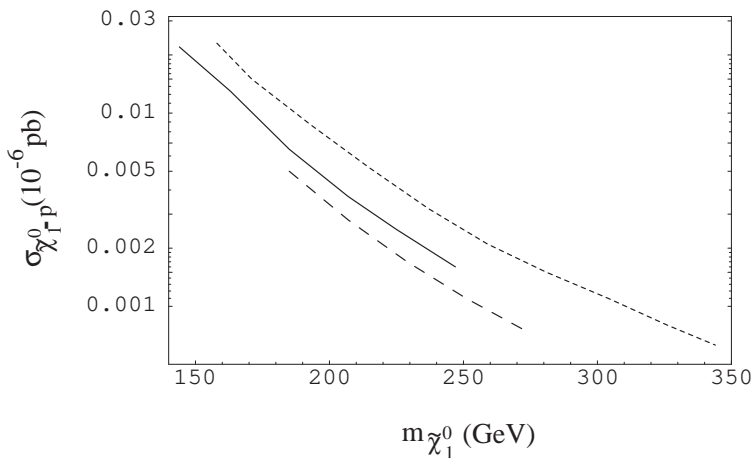


FIG. 2.  $\sigma_{\tilde{\chi}_1^0-p}$  as a function of the neutralino mass  $m_{\tilde{\chi}_1^0}$  for  $\tan\beta = 40$ ,  $\mu > 0$  for  $A_0 = -2m_{1/2}, 4m_{1/2}, 0$  from bottom to top. The curves terminate at small  $m_{\tilde{\chi}_1^0}$  due to the  $b \rightarrow s\gamma$  constraint for  $A_0 = 0$  and  $-2m_{1/2}$  and due to the Higgs mass bound ( $m_h > 111$  GeV) for  $A_0 = 4m_{1/2}$ . The curves terminate at large  $m_{\tilde{\chi}_1^0}$  due to the lower bound on  $a_\mu$  of Eq. (1).

If we reduce  $\tan\beta$ , one might expect the minimum value of  $\sigma_{\tilde{\chi}_1^0-p}$  to significantly decrease. However, the  $a_\mu$  bound then becomes more constraining, eliminating more and more of the high  $m_{1/2}$ , high  $m_0$  region. This is shown in Fig. 3 where the minimum value of  $\sigma_{\tilde{\chi}_1^0-p}$  is plotted as a function of  $m_{\tilde{\chi}_1^0}$ , for  $\tan\beta = 10$ ,  $\mu > 0$ ,  $m_h > 111$  GeV, for  $A_0 = -4m_{1/2}$  (lower curve),  $A_0 = 0$  (upper curve). The  $A_0 = 0$  curve terminates at low  $m_{\tilde{\chi}_1^0}$  due to the Higgs mass bound, while the  $A_0 = -4m_{1/2}$  terminates due to the  $b \rightarrow s\gamma$  constraint. The termination at high  $m_{\tilde{\chi}_1^0}$  is due to the  $a_\mu$  lower bound of Eq. (1). We see that the parameter space is now quite restricted, and so even though  $\tan\beta$  is quite reduced, we find

$\sigma_{\tilde{\chi}_1^0-p} > 4 \times 10^{-10}$  pb. The co-annihilation region begins at  $m_{\tilde{\chi}_1^0} \gtrsim 140$  GeV, and so the earlier part of these curves lie in the non co-annihilation domain.

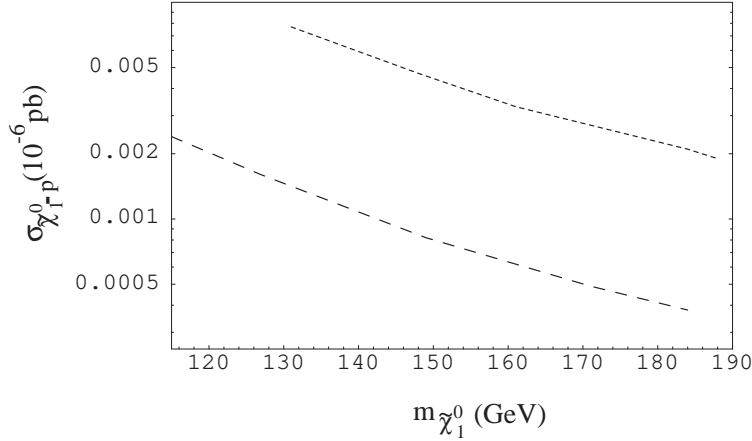


FIG. 3.  $\sigma_{\tilde{\chi}_1^0-p}$  as a function of  $m_{\tilde{\chi}_1^0}$  for  $\tan\beta = 10$ ,  $\mu > 0$ ,  $m_h > 111$  GeV for  $A_0 = 0$  (upper curve),  $A_0 = -4m_{1/2}$  (lower curve). The termination at low  $m_{\tilde{\chi}_1^0}$  is due to the  $m_h$  bound for  $A_0 = 0$ , and the  $b \rightarrow s\gamma$  bound for  $A_0 = -4m_{1/2}$ . The termination at high  $m_{\tilde{\chi}_1^0}$  is due to the lower bound on  $a_\mu$  of Eq. (1).

If we raise  $m_h$  and require  $m_h > 117$  GeV ( corresponding to an experimental bound of 120 GeV), then  $m_h$  controls the termination of the curves at low  $m_{\tilde{\chi}_1^0}$ . Thus for  $\tan\beta = 40$ , the curves of Fig. 2 start at  $m_{\tilde{\chi}_1^0} = 200$  GeV for  $A_0 = -2m_{1/2}$ , at  $m_{\tilde{\chi}_1^0} = 215$  GeV for  $A_0 = 0$ , and at  $m_{\tilde{\chi}_1^0} = 246$  GeV for  $A_0 = 4m_{1/2}$  (i. e. the  $A_0 = 4m_{1/2}$  curve is almost completely eliminated by the  $m_h$  constraint). One has thus only a narrow range of allowed  $m_{\tilde{\chi}_1^0}$ . The allowed range becomes even narrower with decreasing  $\tan\beta$ , and the entire parameter space is eliminated when  $\tan\beta = 10$ .

We turn next to consider non-universal soft breaking models with non-universal masses at  $M_G$  in the third generation squarks and sleptons and in the Higgs masses:

$$\begin{aligned}
m_{H_1}^2 &= m_0^2(1 + \delta_1); & m_{H_2}^2 &= m_0^2(1 + \delta_2); \\
m_{q_L}^2 &= m_0^2(1 + \delta_3); & m_{t_R}^2 &= m_0^2(1 + \delta_4); & m_{\tau_R}^2 &= m_0^2(1 + \delta_5); \\
m_{b_R}^2 &= m_0^2(1 + \delta_6); & m_{l_L}^2 &= m_0^2(1 + \delta_7).
\end{aligned} \tag{4}$$

Here  $\tilde{q}_L = (\tilde{t}_L, \tilde{b}_L)$  squarks,  $\tilde{l}_L = (\tilde{\nu}_\tau, \tilde{\tau}_L)$  sleptons, etc. and we assume  $-1 < \delta_i < +1$ . As discussed in [12], the value of  $\mu$  significantly controls both the relic density and  $\sigma_{\tilde{\chi}_1^0-p}$ , and one may understand qualitatively how  $\mu$  varies from its analytic expression which is valid for low and intermediate  $\tan\beta$ :

$$\begin{aligned}
\mu^2 &= \frac{t^2}{t^2 - 1} \left[ \left( \frac{1 - 3D_0}{2} + \frac{1}{t^2} \right) + \frac{1 - D_0}{2} (\delta_3 + \delta_4) \right. \\
&\quad \left. - \frac{1 + D_0}{2} \delta_2 + \frac{\delta_1}{t^2} \right] m_0^2 + \text{universal parts} + \text{loop corrections}.
\end{aligned} \tag{5}$$

Here  $t = \tan\beta$ , and  $D_0 \cong 1 - (m_t/200 \text{ GeV} \sin\beta)^2 \cong 0.25$ . One sees that the universal  $m_0^2$  term is quite small, and one can easily choose the  $\delta_i$  to make the coefficient of  $m_0^2$  negative.

A reduction of  $\mu^2$  increases the higgsino content of the neutralino, and thus increases the  $\tilde{\chi}_1^0 - \tilde{\chi}_1^0 - Z$  coupling. In [12], it was shown that this allowed the opening of a new region of allowed relic density at high  $m_{1/2}$  and high  $\tan\beta$ . We consider first the simple case where only  $\delta_2$  is non zero and choose  $\delta_2 = 1$ . Fig. 4 shows  $\sigma_{\tilde{\chi}_1^0-p}$  as a function of  $m_{1/2}$  for this case when  $\tan\beta = 40$ ,  $\mu > 0$ ,  $m_h > 111$  GeV and  $A_0 = m_{1/2}$ . The lower line corresponds to the usual stau-neutralino co-annihilation corridor. The upper dashed curves show the new allowed band arising from increased early universe annihilation through the  $Z$  s-channel pole. It is quite broad and has a large scattering cross section. The curves terminate at low  $m_{1/2}$  due to the  $b \rightarrow s\gamma$  constraint, and we have terminated the curves at the high end when  $m_0$  or  $m_{1/2}$  exceed 1 TeV. The vertical lines are the high  $m_{1/2}$  endpoints due to the lower bound on  $a_\mu$  of Eq. (1). One sees that the parameter space is significantly reduced, though there is still a large  $Z$ -channel band remaining. Increasing  $m_h$  increases the lower bound of  $m_{1/2}$ . For  $m_h > 117$  GeV we find the co-annihilation (solid line) now begins at  $m_{1/2} = 510$  GeV, and the  $Z$  channel band begins at 500 GeV due to the  $m_h$  constraint, leaving a sharply reduced region of parameter space.

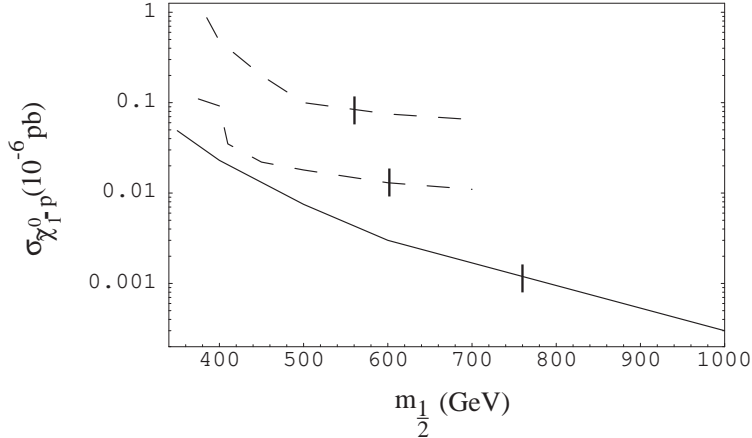


FIG. 4.  $\sigma_{\tilde{\chi}_1^0-p}$  as a function of  $m_{1/2}$  ( $m_{\tilde{\chi}_1^0} \approx 0.4m_{1/2}$ ) for  $\tan\beta = 40$ ,  $\mu > 0$ ,  $m_h > 111$  GeV,  $A_0 = m_{1/2}$  for  $\delta_2 = 1$ . The lower curve is for the  $\tilde{\tau}_1 - \tilde{\chi}_1^0$  co-annihilation channel, and the dashed band is for the  $Z$  s-channel annihilation allowed by non-universal soft breaking. The curves terminate at low  $m_{1/2}$  due to the  $b \rightarrow s\gamma$  constraint. The vertical lines show the termination at high  $m_{1/2}$  due to the lower bound on  $a_\mu$  of Eq. (1).

A second example of new non-universal effects is furnished by choosing  $\delta_{10}$  ( $= \delta_3 = \delta_4 = \delta_5$ ) to be non-zero (as might be the case for an  $SU(5)$  or  $SO(10)$  model). We consider here  $\delta_{10} = -0.7$ . In this case [12] the  $\tilde{\tau}_1 - \tilde{\chi}_1^0$  co-annihilation corridor occurs at a much higher value of  $m_0$  than in the universal case (i. e. for  $m_0 = 600 - 800$  GeV), and is somewhat broadened. The  $Z$  channel band lies above it and is considerably broader. In Fig. 5 we have plotted  $\sigma_{\tilde{\chi}_1^0-p}$  as a function of  $m_{1/2}$  for the lower side of the co-annihilation corridor (lower curve) and for the upper side of the  $Z$  channel band (upper curve) for  $\tan\beta = 40$ ,  $\mu > 0$ ,  $A_0 = m_{1/2}$  and  $m_h > 111$  GeV. (Note that while the  $Z$  channel lies at a higher  $m_0$  in the  $m_0 - m_{1/2}$  plane than the co-annihilation corridor, the cross section is still larger since  $\mu^2$  is reduced.) The curves terminate at the left due to the  $b \rightarrow s\gamma$  constraint. The vertical lines show the termination at high  $m_{1/2}$  due to the lower bound on  $a_\mu$ , significantly shrinking the allowed parameter space. For  $m_h > 117$  GeV, the Higgs mass governs the termination at

low  $m_{1/2}$ , and the co-annihilation (lower curve) now begins at  $m_{1/2} = 515$  GeV, and the  $Z$  channel (upper curve) begins at  $m_{1/2} = 520$  GeV.

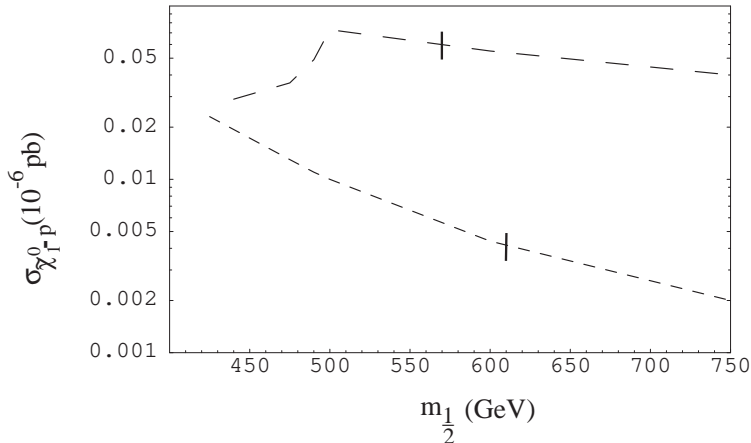


FIG. 5.  $\sigma_{\tilde{\chi}_1^0-p}$  as a function of  $m_{1/2}$  for  $\tan\beta = 40$ ,  $\mu > 0$ ,  $A_0 = m_{1/2}$  and  $m_h > 111$  GeV. The lower curve is for the bottom of the  $\tilde{\tau}_1 - \tilde{\chi}_1^0$  co-annihilation corridor, and the upper curve is for the top of the  $Z$  channel band. The termination at low  $m_{1/2}$  is due to the  $b \rightarrow s\gamma$  constraint, and the vertical lines are the upper bound on  $m_{1/2}$  due to the lower bound of  $a_\mu$  of Eq. (1).

The above discussion shows that for SUGRA models, and particularly for mSUGRA, the  $a_\mu$  data, when combined with the  $m_h$ ,  $b \rightarrow s\gamma$  and relic density constraints have begun to greatly limit the SUSY parameter space. Thus the  $m_h$  and  $b \rightarrow s\gamma$  constraints determine a lower bound on  $m_{1/2}$  and hence an upper bound on  $a_\mu^{\text{SUGRA}}$ , while the experimental lower bound on  $a_\mu$  determines an upper bound on  $m_{1/2}$ . The combined  $a_\mu$  and  $m_h$  bound puts lower bound on  $\tan\beta$  for a given value of  $A_0$ . This can be seen most clearly in Fig. 6, where the mSUGRA contribution to  $a_\mu$  is plotted as a function of  $m_{1/2}$  for  $A_0 = 0$ ,  $\tan\beta = 10$  (lower curve),  $\tan\beta = 30$  (middle curve) and  $\tan\beta = 40$  (upper curve). Further, most of the allowed  $m_{1/2}$  region lies in the  $\tilde{\tau}_1 - \tilde{\chi}_1^0$  co-annihilation domain ( $m_{1/2} \gtrsim 350$  GeV), and so from Fig. 1 one can see that  $m_0$  is approximately determined in terms of  $m_{1/2}$ . In Fig.6, the  $m_h$  bound determines the lower limit on  $m_{1/2}$  for  $\tan\beta=10$ , while  $b \rightarrow s\gamma$  determines it for  $\tan\beta = 40$ . Both are equally constraining for  $\tan\beta = 30$ . If we consider the 90% C. L. bound ( $a_\mu > 21 \times 10^{-10}$ ) [24], one finds for  $A_0 = 0$  that  $\tan\beta \geq 10$ , and for  $\tan\beta \leq 40$  that  $m_{1/2} = (290 - 550)$  GeV, and  $m_0 = (70 - 300)$  GeV. This greatly constrains SUSY particle spectrum expected at accelerators, as can be seen in Table 1. Thus at the 90% C.L. bound on  $a_\mu$  the tri-lepton signal will be unobservable at the Tevatron Run II since  $\tan\beta$  and  $m_{1/2}$  are relatively large [25], and the other SUSY particles are also beyond its reach, except for the light Higgs, provided  $m_h \lesssim 130$  GeV [26]. (One would need to triple the Tevatron's energy to see a significant part of the SUSY mass spectrum.) Only the  $\tilde{\tau}_1$  and  $\tilde{e}_1$  would possibly be within the reach of a 500 GeV NLC (and very marginally the  $\tilde{\chi}_1^\pm$ ), while all the SUSY particles would be accessible to the LHC. The Brookhaven E821 experiment has a great deal more data that can reduce the error by a factor of about 2. When analysed, this would greatly narrow the predictions made here.

One of the interesting features of Fig. 6 is that mSUGRA can no longer accommodate large values of  $a_\mu^{\text{SUGRA}}$ . If the full E821 data should require a value significantly larger than  $40 \times 10^{-10}$ , this would be a signal for the existence of non-universal soft breaking.



From Eq.(3) one sees that one can increase  $a_\mu$  by reducing  $\mu$ , and from Eq. (5) this might be accomplished by non-universal soft breaking of the scalar masses (and also from non-universal gaugino masses at  $M_G$ .) Thus the  $g_\mu - 2$  experiment may give us significant insight into the nature of physics beyond the GUT scale.

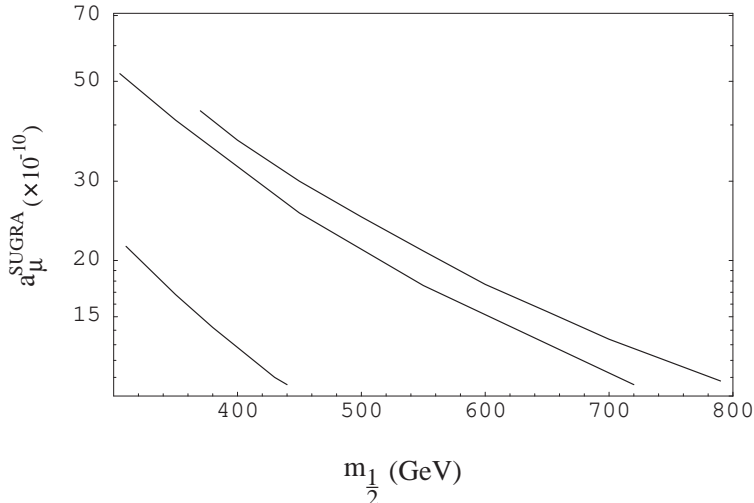


FIG. 6. mSUGRA contribution to  $a_\mu$  as a function of  $m_{1/2}$  for  $A_0 = 0$ ,  $\mu > 0$ , for  $\tan \beta = 10$ , 30 and 40 (bottom to top).

This work was supported in part by National Science Foundation grant No. PHY-0070964.

Table 1. Allowed ranges for SUSY masses in GeV for mSUGRA assuming 90% C. L. for  $a_\mu$  for  $A_0 = 0$ . The lower value of  $m_{\tilde{t}_1}$  can be reduced to 240 GeV by changing  $A_0$  to  $-4m_{1/2}$ . The other masses are not sensitive to  $A_0$ .

$\tilde{\chi}_1^0$	$\tilde{\chi}_1^\pm$	$\tilde{g}$	$\tilde{\tau}_1$	$\tilde{e}_1$	$\tilde{u}_1$	$\tilde{t}_1$
(123-237)	(230-451)	(740-1350)	(134-264)	(145-366)	(660-1220)	(500-940)

## REFERENCES

- [1] H.N. Brown et.al., Muon ( $g-2$ ) Collaboration, hep-ex/0102017.
- [2] P. Fayet, in *Unification of the Fundamental Particle Interactions*, edited by S. Ferrara, J. Ellis, and P. van Nieuwenhuizen (Plenum, New York, 1980); J. A. Grifols and A. Mendez, *Phys. Rev. D* **26**, 1809 (1982); J. Ellis, J. Hagelin and D.V. Nanopoulos, *Phys. Lett. B* **116**, 283 (1982); R. Barbieri and L. Maiani, *Phys. Lett. B* **117**, 203 (1982).
- [3] S. Ferrara and E. Remiddi, *Phys. Lett. B* **53**, 347 (1974).
- [4] A.H. Chamseddine, R. Arnowitt and P. Nath, *Phys. Rev. Lett.* **49**, 970 (1982); R. Barbieri, S. Ferrara and C.A. Savoy, *Phys. Lett. B* **119**, 343 (1982); L. Hall, J. Lykken and S. Weinberg, *Phys. Rev. D* **27**, 2359 (1983); P. Nath, R. Arnowitt and A.H. Chamseddine, *Nucl. Phys. B* **227**, 121 (1983).
- [5] D.A. Kosower, L.M. Krauss and N. Sakai, *Phys. Lett. B* **133**, 305 (1983).
- [6] T.C. Yuan, R. Arnowitt, A.H. Chamseddine and P. Nath, *Z. Phys. C* **26**, 407 (1984).
- [7] U. Chattopadhyay and P. Nath, *Phys. Rev. D* **53**, 1648 (1996); T. Moroi, *Phys. Rev. D* **53**, 6565 (1996); Erratum, *ibid.*, **56**, 4424 (1997). M. Carena, G.F. Giudice and C.E.M. Wagner, *Phys. Lett. B* **390**, 234 (1997); T. Goto, Y. Okada and Y. Shimizu, hep-ph/9908499; T. Blazek, hep-ph/9912460; G.C. Cho, K. Hagiwara and M. Hayakawa, *Phys. Lett. B* **478**, 231 (2000); T. Ibrahim and P. Nath, *Phys. Rev. D* **62**, 015004 (2000).
- [8] A. Czarnecki and W.J. Marciano, hep-ph/0010194.
- [9] J. Ellis, S. Kelley and D.V. Nanopoulos, *Phys. Lett. B* **249**, 441 (1990); U. Amaldi, W de Boer and H. Furstenau, *Phys. Lett. B* **260**, 447 (1991).
- [10] J.L. Lopez, D.V. Nanopoulos and X. Wang, *Phys. Rev. D* **49**, 366 (1994).
- [11] G. Degrassi, P. Gambino and G. Giudice, *JHEP* **0012**, 009 (2000); M. Carena, D. Garcia, U. Nierste and C. Wagner, *Phys. Lett. B* **499**, 141 (2001).
- [12] R. Arnowitt, B. Dutta and Y. Santoso, hep-ph/0102181.
- [13] M. Drees, Y. G. Kim, T. Kobayashi and M. Nojiri, hep-ph/0011359.
- [14] J. Feng and K. Matchev, hep-ph/0102146.
- [15] U. Chattopadhyay and P. Nath, hep-ph/0102157.
- [16] S. Komine, T. Moroi and M. Yamaguchi, hep-ph/0102204.
- [17] J. Ellis, G. Ganis, D.V. Nanopoulos and K.A. Olive, hep-ph/0009355.
- [18] L. Ibanez and C. Lopez, *Nucl. Phys. B* **233**, 511 (1984); V. Barger, M.S. Berger and P. Ohmann, *Phys. Rev. D* **49**, 4908 (1994).
- [19] U. Chattopadhyay and P. Nath, *Phys. Rev. D* **53**, 1648 (1996).
- [20] J. Ellis, A. Ferstl and K.A. Olive, *Phys. Lett. B* **481**, 304 (2000); hep-ph/0007113.
- [21] R. Arnowitt, B. Dutta and Y. Santoso, hep-ph/0010244; hep-ph/0101020.
- [22] M. Gomez and J. Vergados, hep-ph/0012020, M. Gomez, G. Lazarides and C. Pallis, *Phys. Rev. D* **61**, 123512 (2000).
- [23] J. Ellis, T. Falk, G. Ganis, K.A. Olive and M. Srednicki, hep-ph/0102098.
- [24] A. Czarnecki and W.J. Marciano, hep-ph/0102122.
- [25] V. Barger and C. Kao, *Phys. Rev. D* **60**, 115015 (1999); E. Accomando, R. Arnowitt and B. Dutta, *Phys. Lett. B* **475**, 176 (2000).
- [26] M. Carena et.al., “*Report of the Tevatron Higgs Working Group*”, hep-ph/0010338.